Original Article

Efficacy of Luteolin in Mitigating Hyperthyroidism-Induced Structural Changes in the Epididymis of Adult Albino Rats (Histological, Immunohistochemical and Morphometric Study)

Enas Anwar Bekheet and Hala Taha Shalan

Department of Anatomy and Embryology, Faculty of Medicine, Ain Shams University

ABSTRACT

Background: The male epididymis is responsible for storing and maturing sperms. Hyperthyroidism is defined as an increase in the circulating level of thyroid hormones. The change in thyroid hormones level can negatively impact male fertility.

Aim of The Study: The present study aimed to evaluate the effectiveness of luteolin in alleviating the structural changes induced by hyperthyroidism on the epididymis of adult albino rats.

Material and Methods: Forty adult male albino rats were divided into four groups: Group I: IA Subgroup: Rats received no treatment. IB Subgroup: Each rat received 0.5 ml of olive oil via a gastric tube for four weeks. Group II: Each rat received 50 mg/kg of luteolin daily via a gastric tube for four weeks. Group III: Each rat received 100 µg of levothyroxine per kg of body weight daily via a gastric tube for four weeks to induce hyperthyroidism. Group IV: Each rat received levothyroxine as in Group III, along with luteolin as in Group II.

Results: Group III rats exhibited epididymal structural and ultrastructural alterations with significant increase in abnormal sperms, collagen fibers and expressions of PCNA and AR when compared to the control group. In contrast, Group IV rats, showed nearly normal epididymal structural and ultrastructural characteristics with increased collagen fibers and thyroid hormones. However, there was no significant difference in the abnormal sperms number or the expressions of PCNA and AR.

Conclusion: Luteolin may be considered a potential natural adjuvant for treating male infertility, especially in cases linked to oxidative stress, such as hyperthyroidism.

Key Words: Epididymis, hyperthyroidism, luteolin.

Received: 7 January 2025, **Accepted:** 15 February 2025.

Corresponding Author: Enas Anwar Bekheet, Anatomy and Embryology Department, Faculty of Medicine, Ain Shams University, **Tel.:** 01224037554, **E-mail**: eno.anatomy@yahoo.com

ISSN: 2735-3540, Vol. 76, No. 1, March 2025.

INTRODUCTION

The epididymis is a part of male reproductive system responsible for storing and maturing sperms. It consists of three segments: caput (initial segment), corpus (middle segment) and cauda (terminal segment). The caput and corpus are where sperms mature through secretory and absorptive activities of the lining epithelium. The cauda stores mature sperms until ejaculation[1].

Normal blood level of thyroid hormones is crucial for tissues and organs development, growth and function. Increased thyroid hormones level boosts the basal metabolic rate and enhances the production of reactive oxygen species in various cells[2].

Hyperthyroidism is defined as an increase in the circulating level of thyroid hormones (T3, T4) due to an overactive thyroid gland. This condition can result from Grave's disease, thyroiditis, adenomas of the thyroid or pituitary glands or may be iatrogenic. The most common cause is Grave's disease with a global prevalence of 0.5% in men and 2% in women[3].

The change in thyroid hormones level can negatively impact various organs and may result in infertility. In men it negatively impacts male fertility by reducing semen volume, impairing sperms motility and increasing the prevalence of abnormal sperm morphology[4].

DOI: 10.21608/ASMJ.2025.350076.1360

Levothyroxine (L-thyroxine) is a synthetic form of the thyroid hormone T4, commonly used to treat hypothyroidism by supplementing or replacing the hormone. Once administered, it mimics the effects of the natural thyroid hormone in the body[5].

Luteolin is a natural flavonoid found in vegetables, fruits and herbs such as thyme, peppermint, broccoli and apples. It exhibits strong antioxidant, anti-inflammatory, antineoplastic and anti-apoptotic properties through various mechanisms, including scavenging free radicals, chelating ions and protecting against lipid peroxidation. Additionally, luteolin modulates various signaling pathways, gene expression and cellular metabolism. As it is derived from natural sources, luteolin is considered a safe molecule[6-10].

AIM OF WORK

The present study aimed to evaluate the effectiveness of luteolin in alleviating the structural changes induced by hyperthyroidism on the epididymis of adult albino rats.

MATERIALS AND METHODS

Chemicals:

- Levothyroxine (Eltroxin)^{R} tablets (GlaxoSmithKline GmbH, Germany). Each tablet (100µg) was crushed and dissolved in distilled water (2ml) immediately before administration.
- Luteolin (Pure lut)^{R} soft gel capsules (Algonot company, USA). Each capsule (100mg) contained luteolin (98%) dissolved in olive oil (2%). Capsules were evacuated immediately before administration.

Animals:

Forty adult male albino rats were selected with a range of weight from 200-250 gm and age from 7-8 months. Rats were obtained and housed at Medical Research Center (Faculty of Medicine - Ain-Shams University). Rats were hold in metal cages at room temperature with good ventilation and regular light /dark cycles. Access to food and water was freely allowed.

The rats were divided into four equal groups:

- **Control Group (Group I):** It was further subdivided into:
  - Subgroup IA: Rats received no treatment.
  - Subgroup IB: Each rat received 0.5 ml of olive oil via a gastric tube for four weeks.
- **Luteolin Group (Group II):** Each rat received 50 mg/kg of luteolin daily via a gastric tube for four weeks[11].
- **Levothyroxine Group (Group III):** Each rat received 100 µg of levothyroxine per kg of body weight daily via a gastric tube for four weeks to induce hyperthyroidism[12,13].
- **Levothyroxine + Luteolin Group (Group IV):** Each rat received levothyroxine as in Group III, along with luteolin as in Group II for four weeks.

Serum levels of total T3, T4, and TSH were measured before the experiment to confirm that all rats were euthyroid, with normal ranges referenced from ***Sahooa et al.***[14]. Measurements were repeated after four weeks. Enzyme-linked immunosorbent assays (ELISA kits; Monobind, Inc., Costa Mesa, CA, USA) were used for these analyses. Blood samples were collected from each rat's tail vein.

Processing of samples:

Ketamine (60 mg/kg body weight) was administered via intraperitoneal injection for anesthesia. The anterior abdominal wall of each rat was then opened. the caudal region of both epididymides from each rat was dissected and the epididymal contents were gently expressed onto slides for epididymal smear preparation. The samples were subsequently stained with Hematoxylin and Eosin (H&E) to evaluate sperm morphology[15]. Then the corpus region of each epididymis was excised and rinsed with saline. A portion of the specimen was fixed in 10% neutral buffered formalin and processed for paraffin block formation. Another portion was sectioned into small pieces, fixed in 2.5% glutaraldehyde, and processed for Epon block formation.

Cross sections of 5 µm thickness were cut from the paraffin blocks. Sections were stained with H&E[16] for histological examination, Masson trichrome stain to assess collagen fibers[17], immunohistochemical stain for detection of proliferating cell nuclear antigen (PCNA) which is an indicator of cellular proliferation, and immunohistochemical stain for detection of androgen receptor.

For PCNA, a monoclonal anti-PCNA IgG and a biotinylated goat anti-mouse immunoglobulin (Sigma-Aldrich Inc., U.K.) were used. A positive immune reaction was indicated by nuclear brown staining[18]. For androgen receptor (AR), polyclonal anti-AR antibody and a biotinylated goat anti-rabbit immunoglobulin (Sigma-Aldrich Inc., U.K.) were applied. Positive immune reaction appeared as nuclear brown staining[19]. Sections were counterstained with hematoxylin. In negative controls, phosphate-buffered saline replaced the primary antibody. Positive controls for AR were sections from testis and for PCNA, sections were from skin.

Sections from Epon blocks, 1 µm for semithin and 50 nm for ultrathin sections were cut using LKB ultramicrotome. Semithin sections were stained with toluidine blue, while ultrathin sections were stained with uranyl acetate and lead citrate[20].

Stained sections were examined and photographed in the Anatomy Department-Faculty of Medicine-Ain Shams University, using a light microscope with an automatic photomicrographic camera (BX3M series, Olympus, Tokyo, Japan). For ultrathin sections, a transmission electron microscope (Jeol-Ex1010) was used at the Regional Center for Mycology and Biotechnology-Al-Azhar University.

Morphometric Analysis:

Image J software (version 1.48v, National Institute of Health, Bethesda, Maryland, USA) was used for the morphometric analysis. Ten non-overlapping fields from ten different sections of ten distinct rats in the groups I, III, and IV were analyzed to estimate the mean percentage of abnormal sperms per 400 High-power field, the mean area percentage of collagen, the mean area percentage of PCNA and AR expressions and the mean levels of T3, T4 and TSH.

Statistical analysis:

SPSS software (version 20, IBM Corp., Armonk, NY, USA) was used for statistical analysis. Differences between rat groups were compared using one-way ANOVA and Bonferroni post hoc tests. Results were expressed as mean ± standard deviation, with *P-values* displayed in tables and bar charts. *P-values* were categorized as highly significant (≤ 0.001), significant (≤ 0.05) and non-significant (> 0.05).

ETHICAL CONSIDERATION

The study received approval (FMASU R210/2024) from the Research Ethics Committee-Faculty of Medicine-Ain Shams University.

RESULTS

Histological results:

I-Hematoxylin and Eosin (H&E) stained sections:

Examination of cross sections stained with H&E of the epididymides from Group I with its subgroups and Group II rats revealed that the epididymis consisted of multiple tubules, each lined with pseudostratified columnar ciliated epithelium. These tubules were separated by thin connective tissue containing small blood vessels and their lumina were filled with sperms (Figure 1).

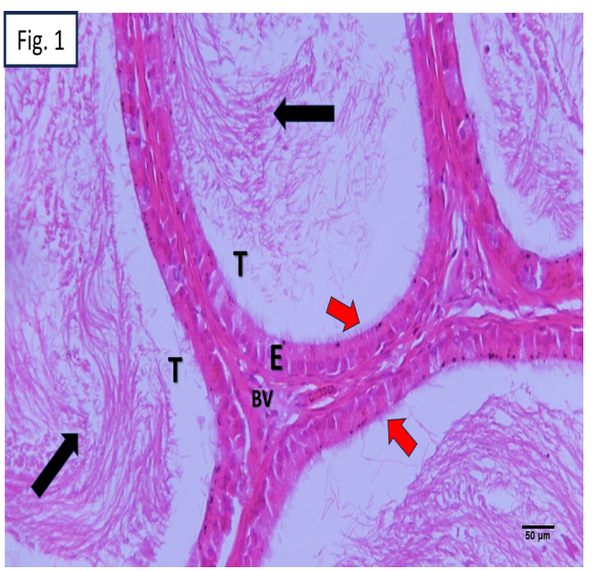

Fig. 1: Microscopic photograph of a cross section from a control rat epididymis showing the epidydimal tubules (T) separated by thin connective tissue containing small blood vessels (BV) and the lumen filled with sperms (black arrows). Notice the pseudostratified columnar epithelium lining of the tubules (E) with brush border (red arrows). (H&E, x200)

Different cell types were clearly distinguished within the epithelium. Principal cells, the most abundant, appeared columnar and eosinophilic extending from the basement membrane to the lumen. They featured stereocilia at their

luminal border, giving a brush border appearance, with rounded to oval, vesicular nuclei aligned at the same level. Clear cells, identified as large, pale-staining cells, were interspersed among the principal cells. Basal cells were having oval nuclei and situated beneath the other cells. (Figure 2).

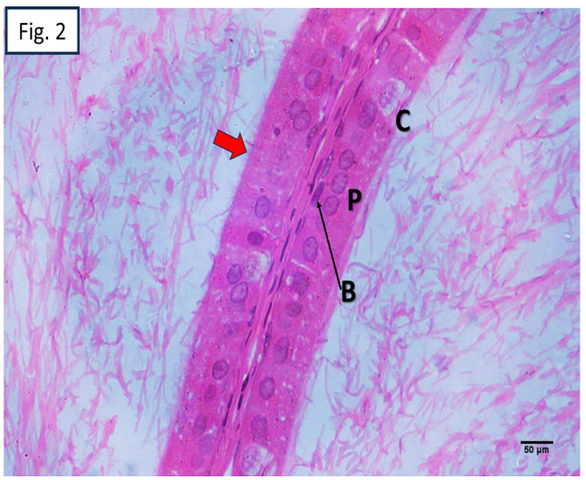

Fig. 2: Microscopic photograph of a cross section of a control rat epididymis showing the principal cells (P) having rounded to oval, vesicular nuclei aligned at the same level and brush border (red arrow). Notice the large, pale-staining clear cell among the principal cells (C) and the basal cell with its oval nucleus (B) beneath the other cells, (H&E, x400)

Examination of the epididymal cross sections from Group III rats revealed irregular lining of the epididymal tubules with regions of disturbed brush border. Some tubules were filled with sperms, others were empty. The epididymal tubules were widely separated by thick connective tissue containing large, congested blood vessels. Additionally, some principal cells showed basal vacuolations and unaligned nuclei (Figures 3,4).

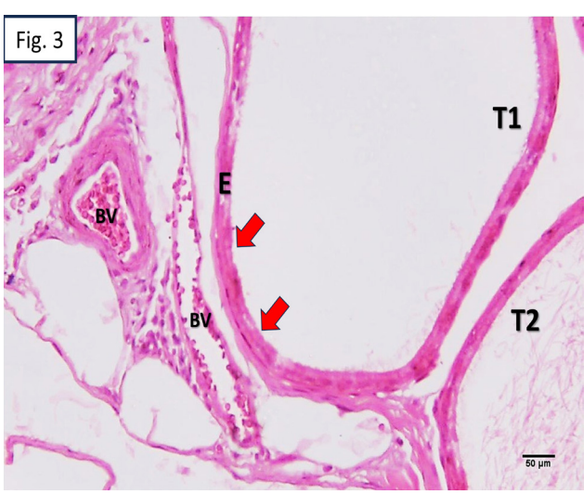

Fig. 3: Microscopic photograph of a cross section of a rat epididymis from Group III showing the irregular lining of the epidydimal tubule (E). The intervening connective tissue containing large, congested blood vessels (BV), Observe a tubule filled with sperm (T2) and another empty one (T1) with regions of disrupted brush border (red arrows). (H&E, x200)

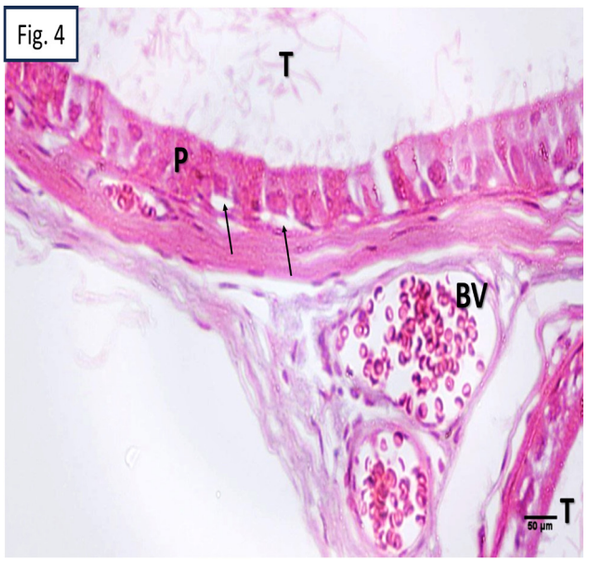

Fig. 4: Microscopic photograph of a cross section of a rat epididymis from Group III showing widely separated epididymal tubules (T) with thick connective tissue containing large, congested blood vessels (BV). Notice the basal vacuolations of some principal cells (arrows) with unaligned nuclei (P). (H&E, x400)

Examination of the epididymal cross sections from Group IV rats revealed nearly regular epididymal tubules filled with sperms, featuring a brush border. These tubules were separated by connective tissue containing small blood vessels. The different cell types within the epithelium were clearly distinguishable (Figures 5,6).

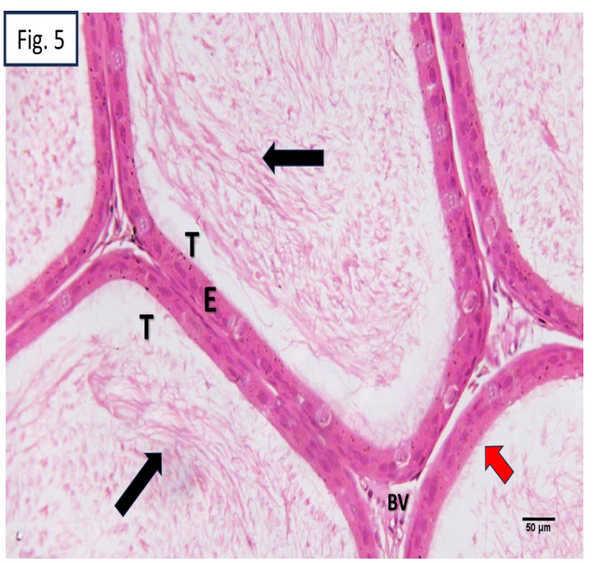

Fig. 5: Microscopic photograph of a cross section of a rat epididymis from Group IV showing the epidydimal tubules (T) separated by connective tissue containing small blood vessels (BV), the lumen filled with sperms (black arrows). Notice the regular lining of the tubules (E) with intact brush border (red arrow). (H&E, x200)

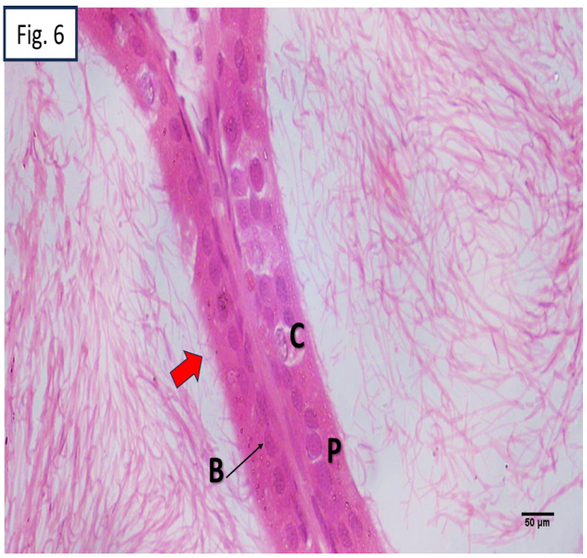

Fig. 6: Microscopic photograph of a cross section of a rat epididymis from Group IV showing clearly distinguishable different cell types, the principal cells with their aligned nuclei (P) and brush border (red arrow), the large, pale-staining clear cells among the principal cells (C), the basal cells with their oval nuclei (B). (H&E, x400)

II- Semithin sections stained with Toluidine blue:

In semithin sections of the Groups I & II, the principal cells displayed vesicular nuclei. The brush border appeared regular with long stereocilia. The clear cells appeared large with light-stained basal nuclei, vesicles of varying sizes and numerous granules. Basal cells appeared with small oval nuclei positioned close to the basement membrane. The cells lay on a well-defined basement membrane (Figure 7).

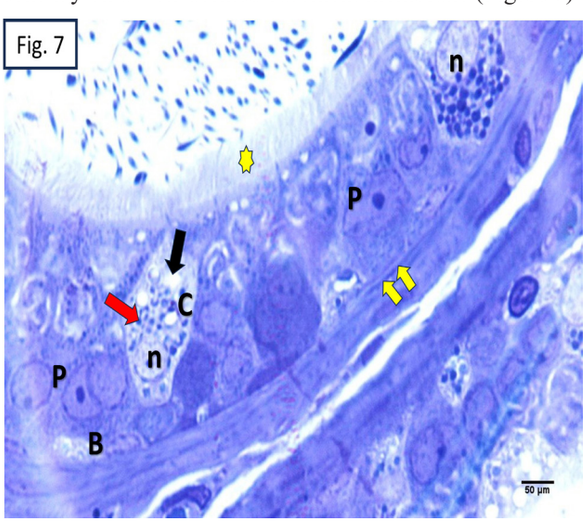

Fig. 7: Microscopic photograph of a cross section of a control rat epididymis showing principal cells display vesicular nuclei (P), clear cells (C) with a light-staining basal nucleus (n) and vesicles of varying sizes (black arrow) in the apical portion, along with numerous granules (red arrow). Basal cell (B) with small oval nucleus positioned close to the basement membrane. Notice the long stereocilia (*) and the well-defined basement membrane (yellow arrows). (Toluidine blue, x1000)

In semithin sections of Group III, principal cells showed light stained nuclei and uneven brush border, while clear cells exhibited basally located nuclei with few granules. Basal cells showed large nuclei with underlying irregular basement membrane (Figure 8).

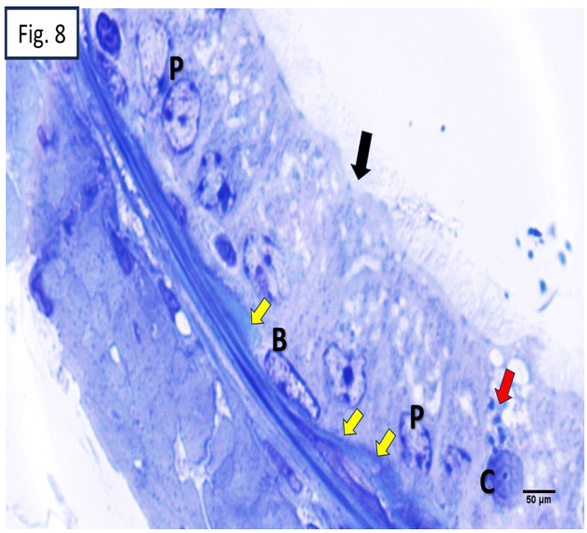

Fig. 8: Microscopic photograph of a cross section of a rat epididymis from Group III showing light stained nuclei of principal cells (P) with uneven brush border (black arrow), clear cell with basal nucleus (C) and few granules (red arrow) and the basal cell having large nucleus (B) with underlying irregular basement membrane (yellow arrows). (Toluidine blue, x1000)

In semithin sections of Group IV, principal cells displayed vesicular nuclei and long stereocilia. The clear cells appeared large with light-stained basal nuclei, vesicles of varying sizes and numerous granules. Basal cells showed small oval nuclei with underlying well-defined basement membrane (Figure 9).

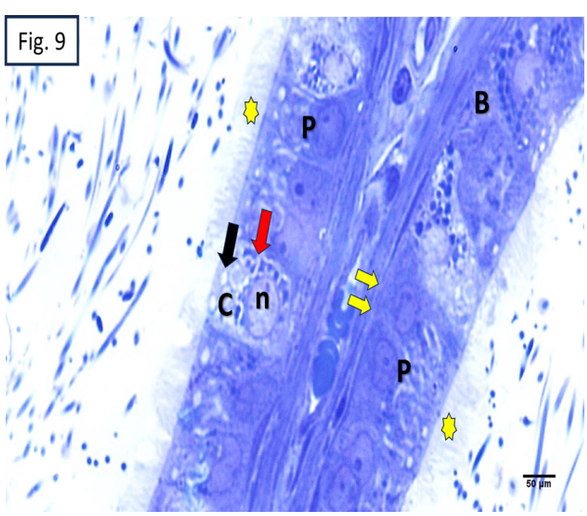

Fig. 9: Microscopic photograph of a cross section of a rat epididymis from Group IV showing the principal cells with vesicular nuclei (P) and long stereocilia (*), the clear cells (C) with a light-stained basal nuclei (n) along with numerous granules (red arrow) and vesicles of varying sizes (black arrow). The basal cell (B) having small oval nucleus with underlying well-defined basement membrane (yellow arrows). (Toluidine blue, x1000)

III- Epididymal smear stained with H&E:

Microscopic examination of the epididymal smears from Groups I&II showed regular structure of most sperms with falciform-shaped heads (hook-like curved head with the base of the head tapered from the neck) and straight tails (Figure 10). The epididymal smears from Group III showed mostly deformed sperms, banana-like heads (uniformly curved head with a broad base that transitions seamlessly into the neck) and irregular tails (Figure 11). Group IV showed mostly regular sperm morphology (Figure 12).

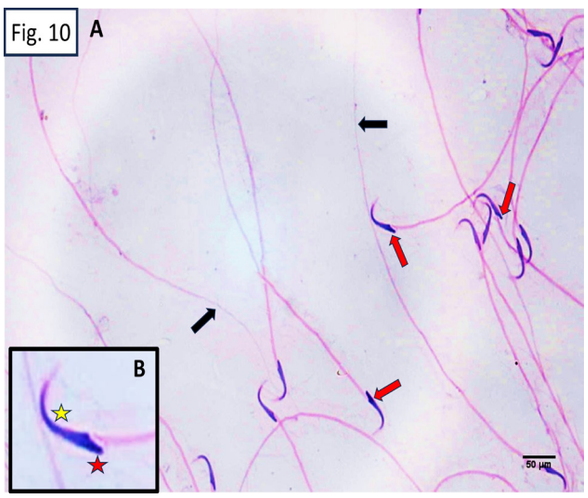

Fig. 10: (A) Microscopic photograph of a control rat epididymal smear showing regular structure of most sperms with falciform-shaped heads (red arrow) and straight tails (black arrow) (H&E, 400x). The insert (B) shows the falciform shaped head, hook-like curve (yellow star) with the base of the head tapered from the neck (red star). (H&E, x1000)

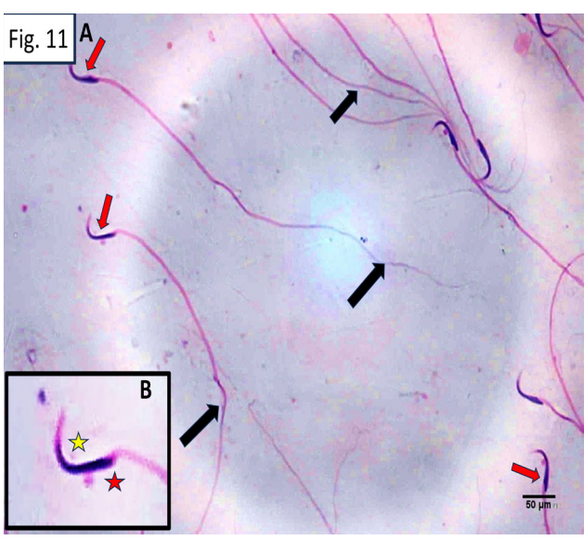

Fig. 11: (A) Microscopic photograph of rat epididymal smear from Group III showing mostly deformed sperms with banana-like heads (red arrows) and irregular tails (black arrows) (H&E, x400). The insert (B) shows the banana shaped head, uniform curve (yellow star) with broad base that transitions seamlessly into the neck (red star). (H&E, x1000)

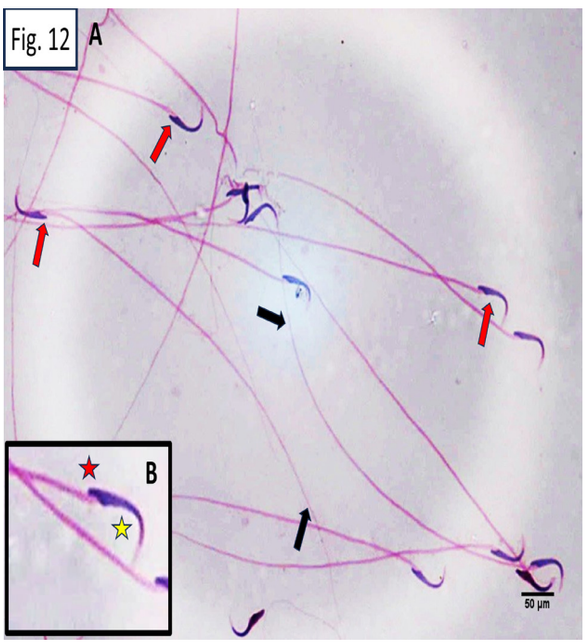

Fig. 12: Microscopic photograph of rat epididymal smear from Group VI showing regular structure of most sperms with falciform-shaped heads (red arrows) and straight tails (black arrows) (H&E, x400). The insert (B) shows the falciform shaped head, hook-like curve (yellow star) with the base of the head tapered from the neck (red star). (H&E, x1000)

IV- Ultrathin sections stained with Uranyl Acetate & Lead Citrate:

Electron microscopic examination of ultrathin sections from Groups I&II epididymides showed principal cell with indented euchromatic nucleus and a prominent nucleolus, the cytoplasm contains regular Golgi apparatus, numerous small mitochondria, lysosomes and apical small vesicles. The clear cell showed euchromatic nucleus with light stained cytoplasm having numerous dark granules of various sizes, large apical vesicles and few small mitochondria. The cells were resting on regular basement membrane lamellae (Figure 13). The lumen was full of cross sectioned sperms at different regions. At higher magnification of cross-sectioned sperms at the midpieces, the sperms displayed a regular structure, including an intact plasma membrane, well-organized mitochondria, properly arranged nine outer dense fibers and a structured axoneme complex (Figures 14,15).

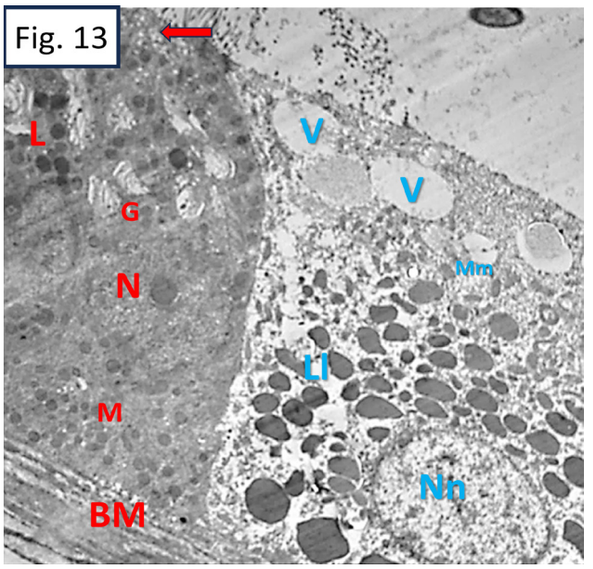

Fig. 13: Electron microscopic photograph of a control rat epididymis showing principal cell having indented euchromatic nucleus with prominent nucleolus (N), the cytoplasm contains regular Golgi apparatus (G), numerous small mitochondria (M), lysosomes (L) and apical small vesicles (red arrow). The clear cell shows euchromatic nucleus (Nn) with light-stained cytoplasm having numerous dark granules (LI) of various sizes, large apical vesicles (V) and few small mitochondria (Mm). The cells resting on regular basement membrane lamellae (BM).
(Uranyl Acetate & Lead Citrate, x2000)

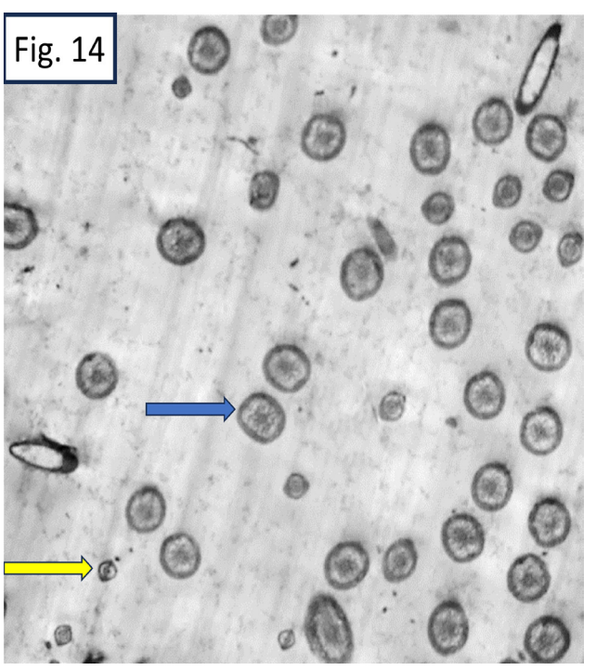

Fig. 14: Electron microscopic photograph from a control rat epididymis showing cross sectioned luminal sperms at different regions, Midpiece (blue arrow) and tail (yellow arrow).
(Uranyl Acetate & Lead Citrate, x2000)

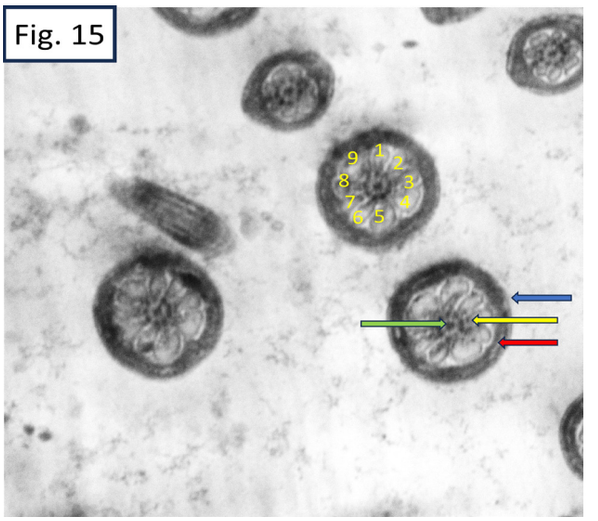

Fig. 15: A higher magnification of the previous electron microscopic photograph of cross section of sperms at the midpiece showing intact plasma membrane (blue arrow) well-organized mitochondria (red arrow), properly arranged nine outer dense fibers (yellow arrow & 1-9) and a structured axoneme complex (green arrow). (Uranyl Acetate & Lead Citrate, x6500)

Ultrathin sections from Group III epididymides revealed principal cells with poorly defined nuclear membranes and the cytoplasm contained dilated Golgi apparatus, scarce mitochondria, lysosomes and apical large vacuoles. The clear cells showed euchromatic nuclei with light-stained cytoplasm having few dark granules and small apical vesicles. The cells were resting on irregular basement membrane lamellae (Figure 16). Cross-sections of sperms at the midpieces revealed structural abnormalities, including a ruptured plasma membrane, fragmented outer dense fibers, degenerated axoneme complex and persistent cytoplasmic droplets (Figure 17).

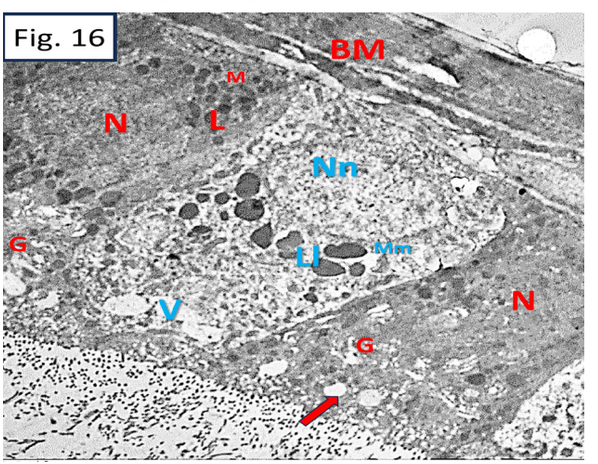

Fig. 16: Electron microscopic photograph from a rat of Group III epididymis showing principal cells with poorly defined nuclear membrane (N), the cytoplasm contains dilated Golgi apparatus (G), scarce mitochondria (M) and lysosomes (L) with apical large vesicles (red arrow). The clear cell shows euchromatic nucleus (Nn) with light stained cytoplasm having few dark granules (LI) and small apical vesicles (V). The cells resting on an irregular basement membrane lamella (BM).
(Uranyl Acetate & Lead Citrate, x2000)

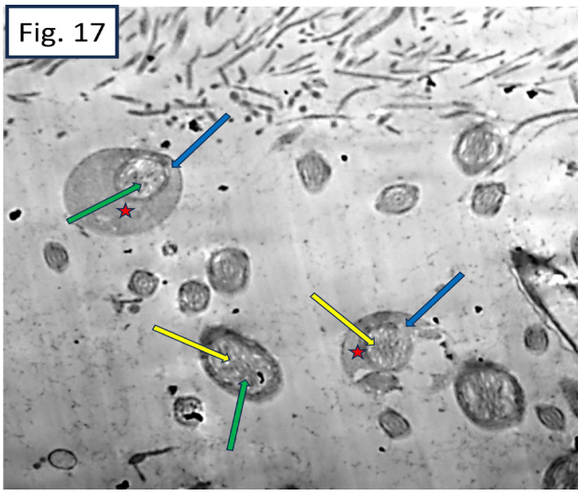

Fig. 17: Electron microscopic photograph of a rat from Group III epididymis showing cross section of sperms at the midpieces with ruptured plasma membrane (blue arrows), fragmented outer dense fibers (yellow arrows) and degenerated axoneme complex (green arrows). Notice the persistent cytoplasmic droplets (*).
(Uranyl Acetate & Lead Citrate, x6500)

Ultrathin sections from Group IV epididymides revealed principal cells with indented euchromatic nuclei and prominent nucleoli and the cytoplasm contained regular Golgi apparatus, many small mitochondria, lysosomes and apical small vesicles. The clear cells showed euchromatic nuclei with light stained cytoplasm having numerous dark granules of various sizes, large apical vesicles and few small mitochondria. The cells were resting on regular basement membrane lamellae (Figure 18). Cross-sectioned sperms at the midpiece displayed a nearly intact plasma membrane, outer dense fibers and axoneme complex (Figure 19).

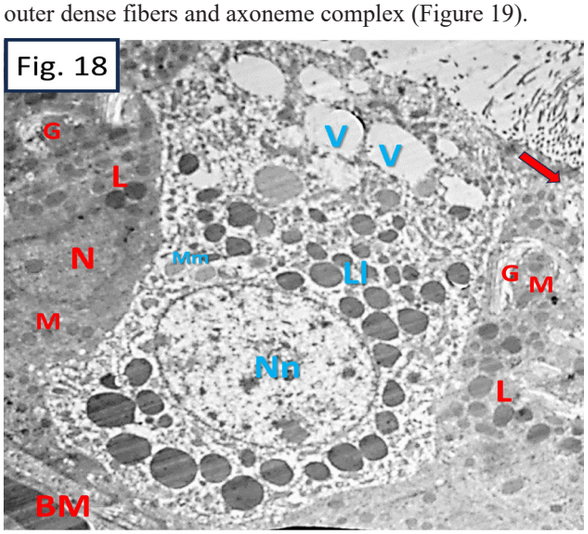

Fig. 18: Electron microscopic photograph of a rat epididymis from Group IV showing principal cell with indented euchromatic nucleus with prominent nucleolus (N), the cytoplasm contains regular Golgi apparatus (G) and many small mitochondria (M), lysosomes (L) and apical small to large vesicles (red arrow). The clear cell shows euchromatic nucleus (Nn) with light stained cytoplasm having numerous dark granules (LI) of various sizes, large apical vesicles (V) and few small mitochondria (Mm). The cells resting on regular basement membrane lamellae (BM).
(Uranyl Acetate & Lead Citrate, x2000)

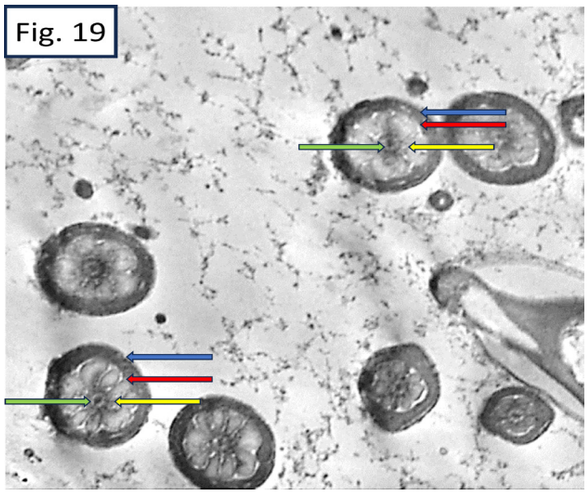

Fig. 19: Electron microscopic photograph from a rat of Group IV epididymis showing cross section of sperms at the midpieces that appeared with intact plasma membrane (blue arrow), well-preserved mitochondria (red arrow), outer dense fibers (yellow arrow) and axoneme complex (green arrow).
(Uranyl Acetate & Lead Citrate, x6500)

V- Masson trichrome stain:

Examination of cross-sections of the epididymides stained with Masson's trichrome stain revealed distinct patterns of collagen fibers arrangement across the groups. Groups I&II showed regular, mesh-like arrangement of few collagen fibers between the tubules (Figure 20). Group III displayed extensive areas of dense collagen fibers between the tubules (Figure 21). Group IV exhibited wide areas of mesh-like arrangement of collagen fibers between the tubules (Figure 22).

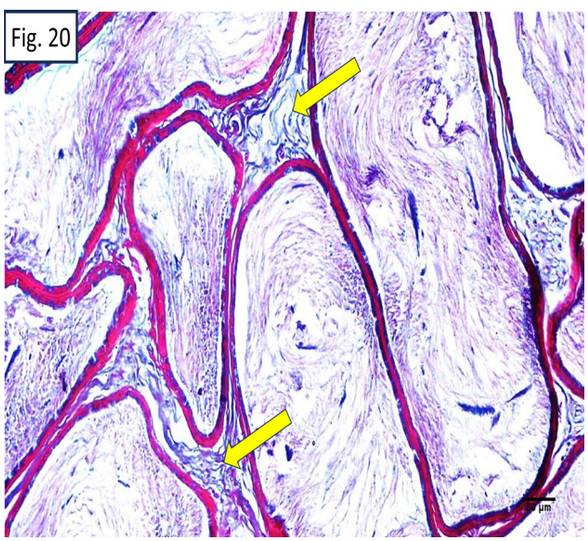

Fig. 20: Microscopic photograph of a cross section of a control rat epididymis showing mesh-like arrangement of few collagen fibers between the tubules (yellow arrows).
(Masson trichrome, x400)

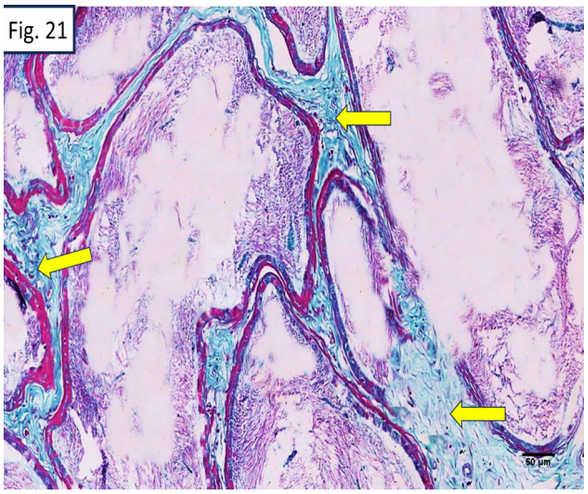

Fig. 21: Microscopic photograph of a cross section of Group III rat epididymis showing extensive areas of dense collagen fibers between the tubules (yellow arrows). (Masson trichrome, x400)

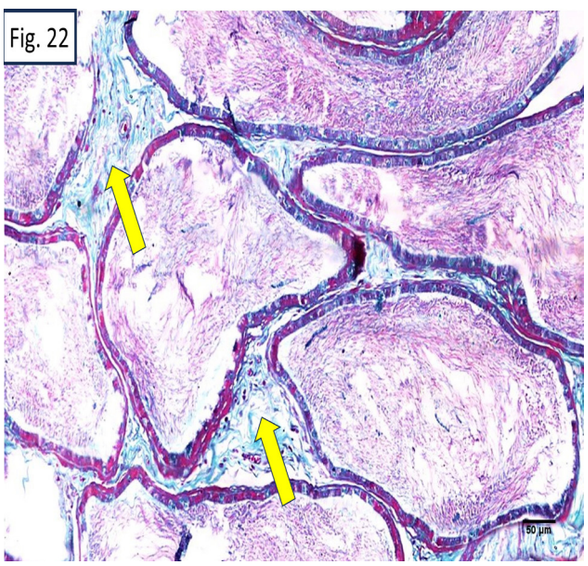

Fig. 22: Microscopic photograph of a cross section from a Group IV rat epididymis showing wide areas of mesh-like arrangement of collagen fibers between the tubules (yellow arrows). (Masson trichrome, x400)

VI- PCNA immunohistochemical stain:

Examination of PCNA immunohistochemically stained epididymal cross sections of Groups I and II revealed a negative nuclear reaction in most of epididymal cells (Figure 23). Group III showed a positive nuclear reaction in the majority of epididymal cells (Figure 24). Group IV displayed a positive nuclear reaction in few epididymal cells (Figure 25).

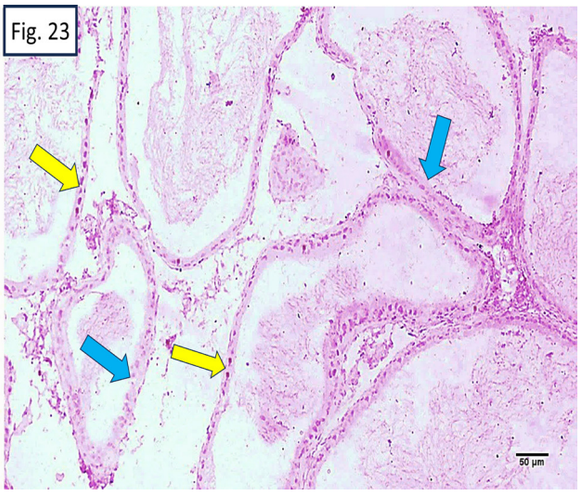

Fig. 23: Microscopic photograph of a cross section from a control rat epididymis showing negative nuclear reaction in most of epididymal cells (blue arrows). Notice, the positive nuclear reaction (yellow arrows) in few scattered epididymal cells. (PCNA, x100)

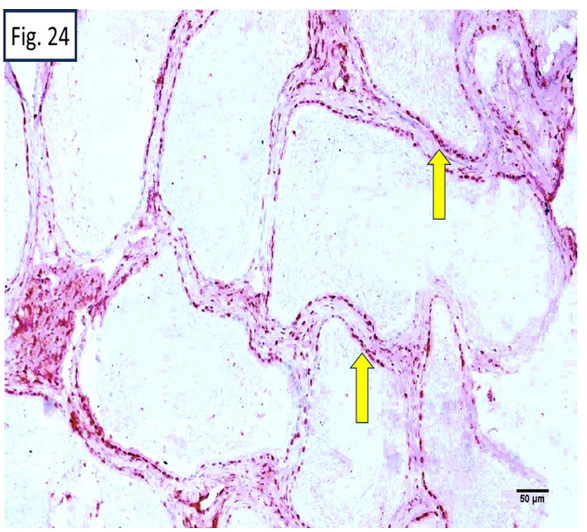

Fig. 24: Microscopic photograph of a cross section from a Group III rat epididymis showing a positive nuclear reaction (yellow arrows) in most of epididymal cells. (PCNA, x100)

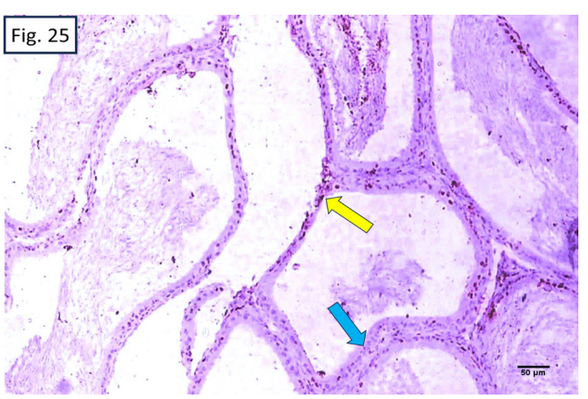

Fig. 25: Microscopic photograph of a cross section from a Group IV rat epididymis showing a negative nuclear reaction in most of epididymal cells (blue arrow) and a positive nuclear reaction (yellow arrow) in few of epididymal cells. (PCNA, x100)

VII- Androgen receptors immunohistochemical stain:

Examination of Groups I&II androgen receptors immunohistochemically stained epididymal cross sections revealed a strong positive nuclear reaction in nearly all epididymal cells (Figure 26). Group III showed a weak positive nuclear reaction in most of epididymal cells (Figure 27). Group IV showed a moderate to strong positive nuclear reaction in most of epididymal cells (Figure 28).

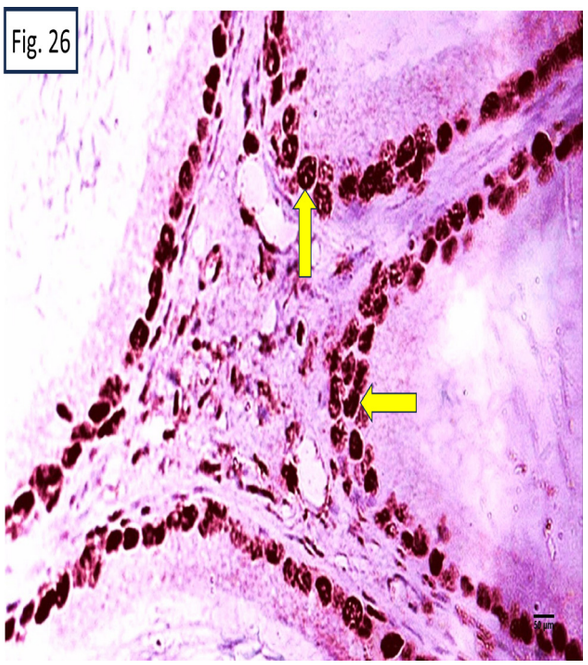

Fig. 26: Microscopic photograph of a cross section from a control rat epididymis showing strong positive nuclear reaction (yellow arrows) in nearly all epididymal cells. (AR, x400)

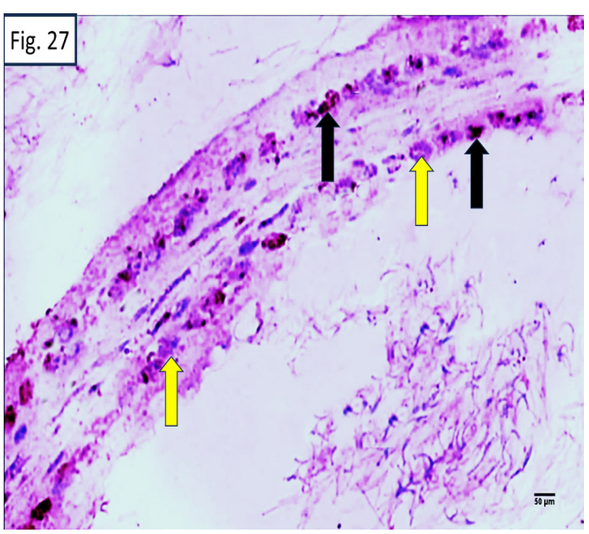

Fig. 27: Microscopic photograph of a cross section from a Group III rat epididymis showing a weak nuclear reaction (yellow arrows) in most of epididymal cells and a moderate nuclear reaction in few of them (black arrows). (AR, x400)

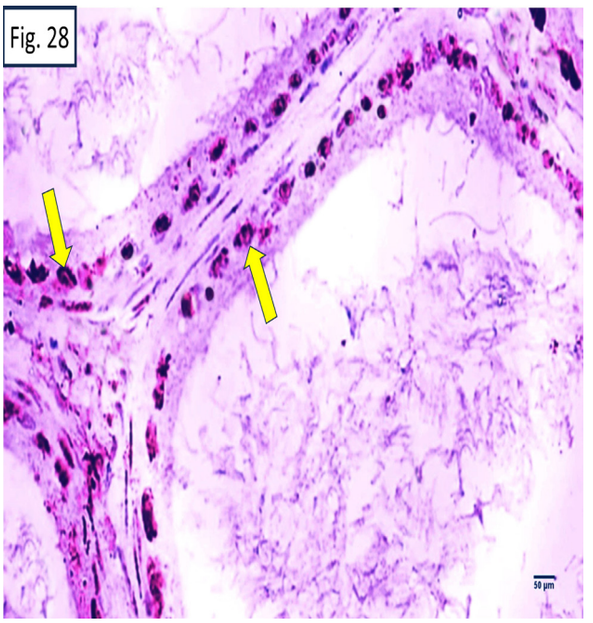

Fig. 28: Microscopic photograph of a cross section from a Group IV rat epididymis showing moderate to strong nuclear reaction (yellow arrows) in most of epididymal cells. (AR, x400)

Statistical analysis: Data were presented in (Tables 1–5) and Bar (Charts 1–5).

-Morphometric Measures

Results showed a highly significant difference in the mean percentage of abnormal sperms per 400 high-power fields, as well as in the mean percentages of PCNA and AR immunohistochemical reactions, between Group I and Group III and between Group III and Group IV. Non-significant difference was found between Group I and Group IV for these measures.

A highly significant difference in the mean area percentage of collagen was identified between Group I and Group III, as well as between Group III and Group IV. Additionally, a significant difference was noted between Group I and Group IV.

-Hormonal Levels

Following L-thyroxine administration, total T3 (ng/ml) and T4 (ng/ml) levels significantly increased in all treated rats of the Groups III and IV compared to Group I. In contrast, TSH (µIU/ml) levels became undetectable in these groups.

Table 1: Comparison between the Groups I, III & IV concerning the mean percentage of abnormal sperms /400 High power field.

	Mean % of abnormal sperms			
	Group I (Control group)	Group III (Levothyroxine group)	Group IV (Levothyroxine + Luteolin group)	*P-value*
Mean ± SD	13±0.35	73±0.20	15±0.05	***$P1 < 0.001$ **$P2 > 0.05$ ***$P3 < 0.001$

*P*1: Group I in contrast with Group III.
*P*2: Group I in contrast with Group IV.
*P*3: Group III in contrast with Group IV.

Significant *P-value* (*) ≤ 0.05.
Non-significant *P-value* (**) > 0.05.
Highly significant *p-value* (***) ≤. 0.001

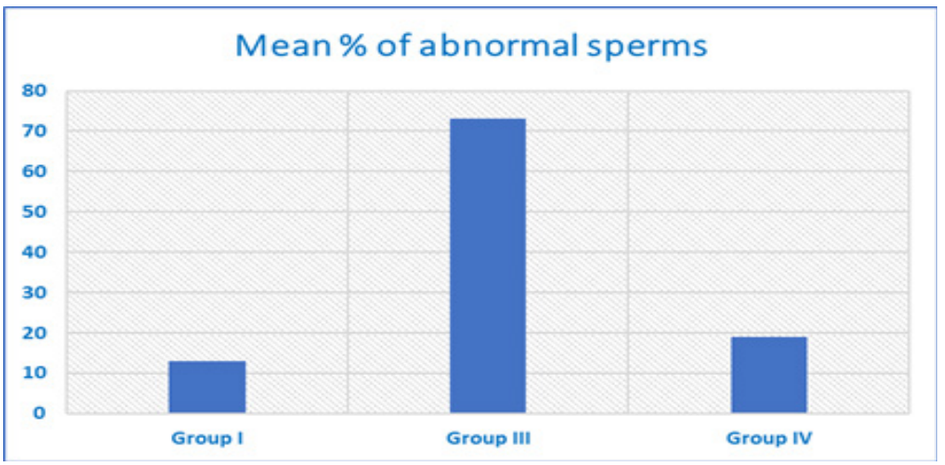

Chart 1: Mean percentage of abnormal sperms /400 High power field.

Table 2: Comparison between the Groups I, III & IV concerning the mean area percentage of collagen fibers.

	Mean area % of collagen fibers			
	Group I (Control group)	Group III (Levothyroxine group)	Group IV (Levothyroxine + Luteolin group)	*P-value*
Mean± SD	30.12±0.39	59.42±0.62	36.56±0.48	***$P1 < 0.001$ *$P2 = 0.01$ ***$P3 < 0.001$

*P*1: Group I in contrast with Group III.
*P*2: Group I in contrast with Group IV.
*P*3: Group III in contrast with Group IV.

Significant *P-value* (*) ≤ 0.05.
Non-significant *P-value* (**) > 0.05.
Highly significant *p-value* (***) ≤. 0.001

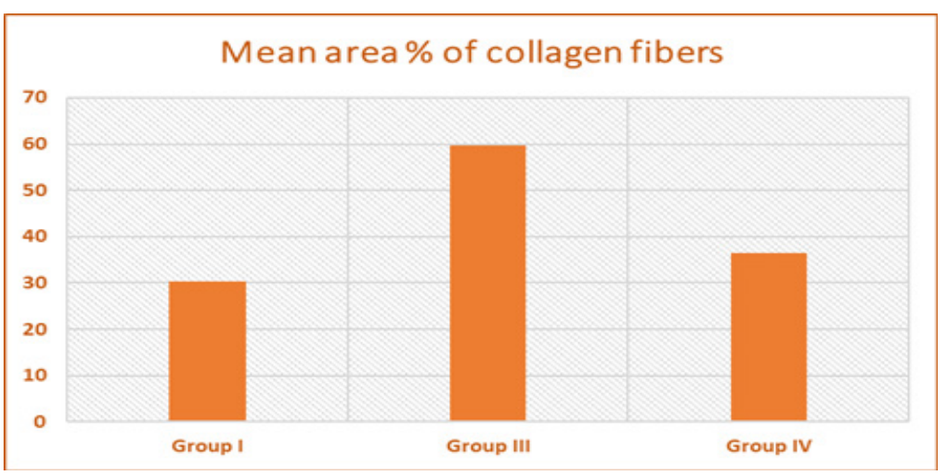

Chart 2: Mean area % of collagen fibers.

Table 3: Comparison between the Groups I, III & IV groups concerning the mean area percentage of PCNA expression.

	Mean area % of PCNA			
	Group I (Control group)	Group III (Levothyroxine group)	Group IV (Levothyroxine + Luteolin group)	*P-value*
Mean± SD	3.56±0.04	77.36±0.03	4.95±0.12	***P1 < 0.001 **P2 > 0.05 ***P3 < 0.001

*P*1: Group I in contrast with Group III.
*P*2: Group I in contrast with Group IV.
*P*3: Group III in contrast with Group IV.
Significant *P-value* (*) ≤ 0.05.
Non-significant *P-value* (**) > 0.05.
Highly significant *p-value* (***) ≤. 0.001

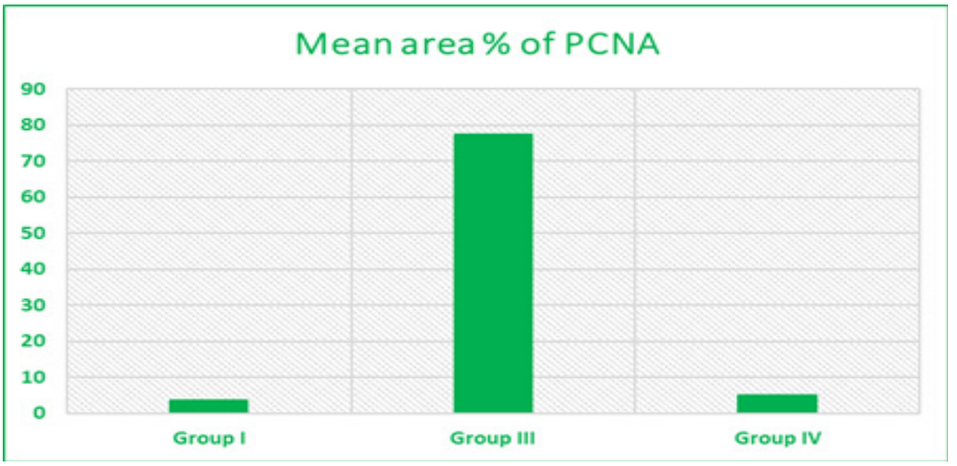

Chart 3: Mean area % of PCNA expression.

Table 4: Comparison between the Groups I, III & IV concerning the mean area percentage of AR expression.

	Mean area % of AR			
	Group I (Control group)	Group III (Levothyroxine group)	Group IV (Levothyroxine + Luteolin group)	*P-value*
Mean ± SD	82.49±0.07	27.30±0.17	79.08±0.05	***P1 < 0.001 **P2 > 0.05 ***P3 < 0.001

*P*1: Group I in contrast with Group III.
*P*2: Group I in contrast with Group IV.
*P*3: Group III in contrast with Group IV.
Significant *P-value* (*) ≤ 0.05.
Non-significant *P-value* (**) > 0.05.
Highly significant *p-value* (***) ≤. 0.001

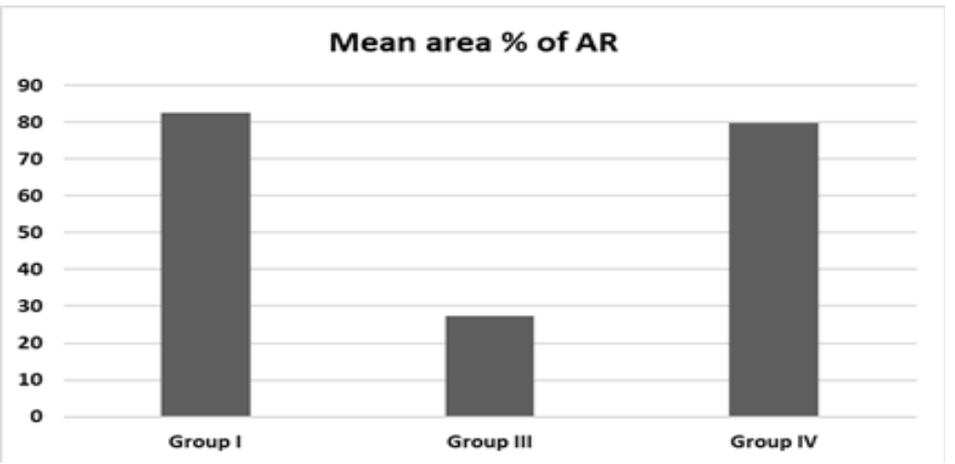

Chart 4: Mean area % of AR expression.

Table 5: Comparison between the Groups I, III & IV concerning T3, T4 and TSH levels.

	Mean T3, T4 and TSH levels			
	Group I (Control group)	Group III (Levothyroxine group)	Group IV (Levothyroxine + Luteolin group)	*P-value*
Mean ± SD				
T3	0.4 ± 0.1	1.2 ± 0.1	1.0±0.2	***P1 < 0.001
T4	32.1 ± 1.0	150.2 ± 0.2	148.3±0.1	***P2 < 0.001
TSH	0.1 ± 0.1	Undetectable	Undetectable	**P3 > 0.05

*P*1: Group I in contrast with Group III.
*P*2: Group I in contrast with Group IV.
*P*3: Group III in contrast with Group IV.

Significant *P-value* (*) ≤ 0.05.
Non-significant *P-value* (**) > 0.05.
Highly significant *p-value* (***) ≤. 0.001

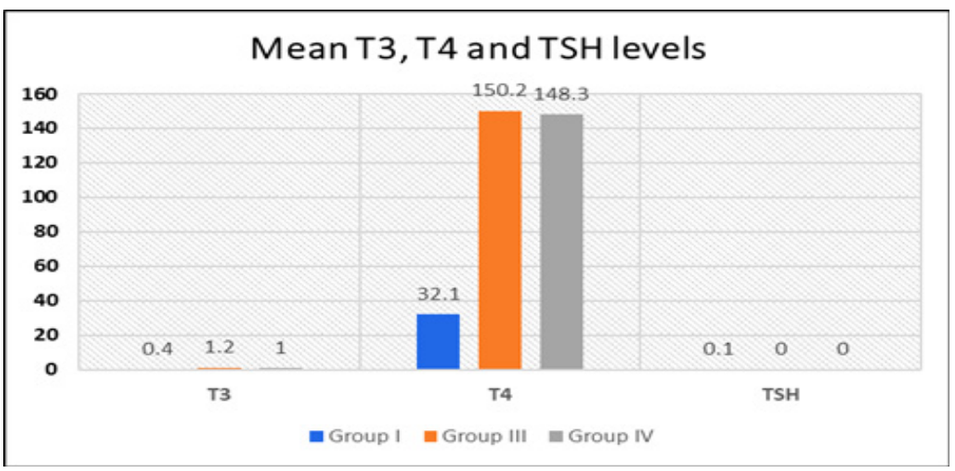

Chart 5: Mean T3, T4 and TSH levels.

DISCUSSION

The present study examined the effectiveness of luteolin in mitigating the structural effects of hyperthyroidism on the epididymis of adult albino rats.

Research on hyperthyroidism in male rats has predominantly concentrated on its impact on the testes. However, the epididymis plays an essential role in male fertility[21].

In this study, after four weeks of levothyroxine administration, Group III rats exhibited significantly elevated total T3 and T4 levels compared to the control group, with undetectable TSH levels, indicating hyperthyroidism[14]. Histological analysis revealed the adverse impact of hyperthyroidism on the epididymal structure. The lining of the epididymal tubules appeared irregular with focal loss of the brush border. Most tubules exhibited depletion of sperms. The tubules were widely separated by thickened connective tissue containing large, congested blood vessels. These changes are consistent with the findings of ***Korejo et al.***[22], who linked similar alterations to a deficiency in androgen hormones.

Hyperthyroidism can reduce androgen levels through several mechanisms: directly by affecting Leydig cells, leading to decreased testosterone production; indirectly by disrupting the hypothalamic-pituitary-gonadal axis, which suppresses the release of gonadotropins (LH and FSH) necessary for testosterone synthesis and by increasing the conversion of testosterone to estrogen via the enzyme aromatase. These factors collectively contribute to a relative androgen deficiency[23,24].

Hyperthyroidism adversely affects the principal cells of the epididymis, leading to both structural and ultrastructural disruptions, as observed in the present study. These disruptions include basal vacuolation of some principal cells with misaligned nuclei, dilated Golgi apparatus and alongside irregularities in the basement membrane lamellae. Such alterations suggest cellular stress and dysfunction, likely due to oxidative stress, as reported in a previous study[25].

In the present study, hyperthyroidism induced several ultrastructural changes in clear cells, including a reduction in their secretory granules, which suggest cellular stress, potentially impairing the clear cells' ability to secrete and absorb fluids. Such dysfunction could disrupt sperm

maturation and overall epididymal function. Additionally, the basal cells exhibited large nuclei. Basal cells play a crucial role in producing prostaglandins that regulate water and electrolyte transport by the principal cells. They also protect maturing sperm in the epididymis by defending against reactive oxygen species[26,27].

Moreover, histological examination and statistical analysis revealed a significant increase in sperms' head and tail abnormalities. Ultrastructural examination of the midpiece revealed ruptured membranes, degenerated axoneme complexes, fragmented outer dense fibers and persistent cytoplasmic droplets. ***Hegazy et al.***[28] reported that levothyroxine administration in rats significantly impacts testicular structure and increases the incidence of abnormal sperm forms.

Cytoplasmic droplets around the midpiece should be fully eliminated by the time sperms reach the epididymis. The presence of these droplets in many sperm indicates immaturity or dysfunction. Thyroid hormones may directly affect sperms by binding to non-nuclear receptors located in the cell membrane, cytoplasm and mitochondria[29].

The axoneme complex, a critical part of the sperm's cytoskeleton, consists of microtubules organized into ten doublets, one central doublet and nine arranged in a surrounding circle. This structure is essential for motility, signaling and energy supply. This complex is reinforced by nine dense outer fibers that stabilize the structure and support mitochondria in the midpiece, ensuring efficient ATP production for movement. Although sperms are produced in the testis, they are initially nonfunctional and require maturation in the epididymis to acquire motility and the ability to fertilize an ovum[30-32].

In the same context, a highly significant increase in collagen fibers and cellular proliferation, along with a highly significant reduced expression of androgen receptors in the epididymides of Group III was found compared to the control group. These alterations may be attributed to elevated mitochondrial metabolism and an increase in reactive oxygen species, leading to oxidative stress. This stress likely damages cellular structures and androgen receptors, resulting in reduced receptor sensitivity or expression. Moreover, oxidative stress may stimulate excessive collagen fibers production, as reported in previous studies[33,34].

The epididymis is highly dependent on androgens for its function and structural integrity. Androgen receptors in the epididymis play a crucial role in maintaining the epididymal environment necessary for sperms to acquire motility and fertilizing potential. In epithelial cells, androgen receptors activation regulates the secretion of proteins and ions that contribute to the maturation and storage of sperm. In the stromal compartment, androgen signaling helps sustain the supportive tissue architecture and vascularization needed for optimal epididymal function[21]. High levels of thyroid hormones may affect the transcription and expression of genes responsible for androgen receptor production[35].

Elevated thyroid hormones stimulate various cellular processes, including mitosis and tissue remodeling. This can result in enhanced cellular proliferation, particularly in tissues like the epididymis, which are sensitive to hormonal changes. In the case of hyperthyroidism, this proliferation is often a response to the increased oxidative stress and altered metabolic activities. Hyperthyroidism can disrupt mitochondrial function and redox balance in reproductive organs, including the testis and epididymis. This disruption may cause alterations in cell growth and division, potentially leading to an increased number of cells as the body attempts to cope with oxidative damage[36].

In this study, after four weeks of combined L-thyroxine and Luteolin administration in Group IV rats, they exhibited a highly significant elevated total T3 and T4 levels, similar to Group III with undetectable TSH levels, compared to the control group. This suggests that Luteolin had no effect on thyroid hormone levels, as the combination of levothyroxine and luteolin did not modify the elevated thyroid hormone status induced by levothyroxine alone. In addition, when luteolin was administered alone in Group II rats, microscopic examination of the epididymis and thyroid hormone levels were the same as those in the control group.

Structural and ultrastructural analysis of the epididymis in Group IV rats revealed nearly regular sperm filled tubules. The tubules were separated by connective tissue containing small blood vessels. The epithelial principal cells showed vesicular nuclei with long stereocilia. The clear cells showed light-stained basal nuclei, large vesicles and numerus granules. The basal cells exhibited small oval nuclei. Sperms predominantly displayed regular morphology with intact plasma membranes, mitochondria, outer dense fibers and axoneme complexes of their midpieces.

Ultrastructural examination showed principal cells with euchromatic, indented nuclei, prominent nucleoli and cytoplasm containing a well-defined Golgi apparatus, small mitochondria, lysosomes and apical vesicles. Clear cells had euchromatic nuclei, lightly stained cytoplasm with dark granules, large apical vesicles and few small mitochondria, while basal cells had small oval nuclei.

A recent study has explored the therapeutic potential of plant-derived compounds, particularly luteolin, a flavonoid found in citrus fruits and vegetables[37]. Another study revealed that luteolin treatment increased sperm count and serum testosterone levels in rats[38]. Further study demonstrated that luteolin provided protection against testicular damage, oxidative stress and inflammation in rats exposed to lead acetate[39].

Animal studies suggest that luteolin can protect spermatogenesis by promoting healthy cell cycles and preventing germ cells apoptosis in testes, potentially enhancing sperm production and quality. Luteolin may also improve sperm quality by reducing DNA fragmentation and improving motility, especially in cases of oxidative stress affecting sperm's function[40].

In Group IV, collagen fiber density decreased noticeably with a significant difference in contrast with Group III. Luteolin's has a well-known anti-fibrotic effect, which enhance the production of NO and cGMP. The NO-cGMP pathway aids in reducing collagen fiber production and growth. Furthermore, there was no significant difference in cellular proliferation, androgen receptor expression or the number of abnormal sperms when compared to the control group[41].

Luteolin has shown potential benefits for epididymal cells, primarily through its antioxidant and anti-inflammatory properties. These effects may support a healthier environment for sperm maturation and maintaining the integrity of epididymal tissue. Through these protective mechanisms, luteolin may indirectly enhance sperm quality, particularly in terms of motility and structural integrity, which could be beneficial for male fertility, especially in cases where oxidative stress or inflammation impacts epididymal function[42].

CONCLUSION

Luteolin may be considered a potential natural adjuvant for treating male infertility, especially in cases linked to oxidative stress, such as hyperthyroidism.

CONFLICT OF INTERESTS

There is no conflicts of interest.

AUTHORS CONTRIBUTION

Both authors participated equally and collaboratively in all stages of the research, which included:

DEVELOPING THE RESEARCH IDEA AND PREPARING ITS PLAN

By discussing the objectives and designing a comprehensive methodology.

COLLECTING SCIENTIFIC MATERIALS

Reviewing previous studies and relevant references to establish a solid scientific foundation.

CONDUCTING THE PRACTICAL WORK

Performing experimental procedures and analyzing samples with precision.

ANALYZING AND STATISTICALLY INTERPRETING THE RESULTS

To derive accurate conclusions based on scientific principles.

WRITING AND PREPARING THE RESEARCH FOR PUBLICATION

Drafting scientific texts and formatting them according to academic journal standards.

REVIEWING THE TEXT AND REFERENCES

Ensuring linguistic accuracy, proper citation, and overall content quality.

REFERENCES

1. **Ahmed MH, Sabry SM, Zaki SM, El-Sadik AO (2009):** Histological, immunohistochemical and ultrastructural study of the epididymis in the adult albino rat. Aust J Basic Appl Sci. 3(3):2278-2289.

2. **Jahnke GD, Neepa Y. Moore CJA and Shelby MD (2014):** Thyroid Toxicants: Assessing Reproductive Health Effects,112(3):362-368.

3. **Guyton AC and Hall JE (2011):** Guyton and Hall Textbook of Medical Physiology. 12th edition, Philadelphia, Pp: 907-916.

4. **La Vignera S and Vita R (2018):** Thyroid dysfunction and semen quality. International Journal of Immunopathology and Pharmacology. (32): 1–5.

5. **Benvenga S and Carlé A (2019):** Levothyroxine formulations: pharmacological and clinical implications of generic substitution. Adv Ther., 36: 59–71.

6. **Imran M, Rauf A, Abu-Izneid T, Nadeem M, Shariati MA, Khan IA *et al.* (2019):** Luteolin, a flavonoid, as an anticancer agent: a review. Biomedicine & Pharmacotherapy, 112:1-10.

7. **Ekpo DE, Joshua PE, Ogidigo JO and Nwodo OFC (2020):** High resolution UPLC-PDA-QTOF-ESI-MS/MS analysis of the flavonoid rich fraction of Lasianthera africana leaves, and in vivo evaluation of its renal and cardiac function effects. Heliyon, 6: 1-12.

8. **Kwon EY and Choi MS (2018):** Luteolin targets the toll-like receptor signaling pathway in prevention of hepatic and adipocyte fibrosis and insulin resistance in diet-induced obese mice. Nutrients, 10:1-17.

9. **Caporali S, De-Stefano A, Calabrese C, Giovannelli A, Pieri M, Savini *et al.* (2022):** Anti-Inflammatory and Active Biological Properties of the Plant-Derived Bioactive Compounds Luteolin and Luteolin 7-Glucoside. Nutrients, 14(6):1-19.

10. **Muruganathan N, Dhanapal AR, Baskar V, Muthuramalingam P, Selvaraj D, Aara H *et al.* (2022):** Recent Updates on Source, Biosynthesis, and Therapeutic Potential of Natural Flavonoid Luteolin: A Review. Metabolites,12:1-18.

11. **Albrahim T, Robert A, Owumi SE, Ijadele AO, Arunsi UO and Odunola OA (2020):** Luteolin abates reproductive toxicity mediated by the oxido-inflammatory response in doxorubicin-treated rats. Toxicology research and application, 9(4):1-16.

12. **Albrahim T and Robert A (2020):** Renal protective effects of grape seed extract treatment against Eltroxin-induced hyperthyroidism, kidney damage, and oxidative stress in male mice. Environmental Science and Pollution Research, 27:17963–17971.

13. **Maran RRM, Priyadarsini D, Udhayakumar RCR, Arunakaran J and Aruldhas MM (2001):** Differential effect of hyperthyroidism on rat epididymal glycosidases. international journal of andrology, 24:206-215.

14. **Sahooa DK, Roya AB and Chainya GBN (2008):** Protective effects of vitamin E and curcumin on l-thyroxine-induced rat testicular oxidative stress. Chemico-Biological Interactions 176:121-128.

15. **Dibal NI, Garba SH and Jacks TW (2020):** Morphological assessment of epididymal sperm in Wistar rats using different histological stains. Acta Veterinaria Eurasia, 1;46(3):132-7.

16. **Kiernan JA (2015):** Histological and Histochemical Methods: Theory and Practice 5th edition, Scion Publishing Ltd, Banbury, UK. pp 571.

17. **Chandler N (2009):** The Masson trichrome staining methods in routine laboratory use. Stain technology journal, 8(3): 101-110.

18. **Jackson P and Blythe D (2013):** Immunohistochemical techniques. Suvarna SK, Layton C, Bancroft JD, editors. Chapter 8: Theory and practice of histological techniques. 7th ed. Philadelphia: Churchill Livingstone of Elsevier. p381–434. Doi.org/10.1016/B978-0-7020-4226-3.00018-4.

19. **Buchwalow, IB and Böcker, W (2010):** Immunohistochemistry: Basics and Methods.Springer, Heidelberg, Dordecht, London, New York, pp. 31–39.

20. **Reynolds ES (1963):** The use of lead citrate of high pH as an electron opaque stain in electron microscopy. J cell Biol., 17: 208-240.

21. **Zhu Li-Ji, Hardy MP, Inigo IV, Huhtaniemi I, Bardin CW and Young AJM (2000):** Effects of Androgen-on-Androgen Receptor Expression in Rat Testicular and Epididymal Cells: A Quantitative Immunohistochemical Study, Biology of Reproduction. 63(2):368–376.

22. **Korejo NZ, Wei Q-W, AShah AH and Shi F-X (2016):** Effects of concomitant diabetes mellitus and hyperthyroidism on testicular and epididymal histoarchitecture and steroidogenesis in male animals. Journal of Zhejiang University-SCIENCE B (Biomedicine & Biotechnology). 17(11):850-863

23. **Krassas GE, Poppe K and Glinoer D (2010):** Thyroid function and human reproductive health. Endocr Rev. 31(5):702–755.

24. **Maran R (2003):** Thyroid hormones: their role in testicular steroidogenesis. Arch Androl. 49(5):375–388.

25. **Wu PY, Scarlata E and O'Flaherty C (2020):** Long-Term Adverse Effects of Oxidative Stress on Rat Epididymis and Spermatozoa. Antioxidants. 2020 Feb 19;9(2):170.

26. **Battistone MA, Elizagaray ML, Barrachina F, Ottino K, Mendelsohn AC, Breton S (2024):** Immunoregulatory mechanisms between epithelial clear cells and mononuclear phagocytes in the epididymis. Andrology. 12: 949–963.

27. **Breton S, Ruan YC, Park YJ, Kim B (2016):** Regulation of epithelial function, differentiation, and remodeling in the epididymis. Asian J Androl. 18(1):3-9.

28. **Hegazy, AA, Morsy MM, Moawad RS and Elsayed GM (2020):** Histological study on the effect of experimentally induced hyperthyroidism on testes of adult albino rats and possible ameliorating role of L-carnitine." Egyptian Journal of Histology 43: 63-74.

29. **La Vignera S and Vita R. (2018):** Thyroid dysfunction and semen quality. Int J Immunopathol Pharmacol. 32:1-5.

30. **Lin YW, Hsu TH and Yen PH (2013):** Mouse sperm acquire a new structure on the apical hook during epididymal maturation. Asian J Androl. 15(4):523-528.

31. **Zhao W, Li Z, Ping P, Wang G, Yuan X and Sun F (2018):** Outer dense fibers stabilize the axoneme to maintain sperm motility. J Cell Mol Med. 22(3):1755-1768.

32. **Guseva EA, Buev VS, Mirzaeva SE, Pletnev PI, Dontsova OA and Sergiev PV (2024):** Structure and Composition of Spermatozoa Fibrous Sheath in Diverse Groups of Metazoa. International Journal of Molecular Sciences. 25(14):1-22.

33. **Kim SM, Kim SC, Chung IK, Cheon WH and Ku SK (2012):** Antioxidant and protective effects of bupleurum falcatum on the L-thyroxine-induced hyperthyroidism in rats. Evid Based Complement. 2012: 3-6.

34. **Fasciolo G, Napolitano G, Aprile M, Cataldi S, Costa V, Muscari Tomajoli MT, Lombardi A, Di Meo S and Venditti P (2023):** Muscle Oxidative Stress Plays a Role in Hyperthyroidism-Linked Insulin Resistance. Antioxidants. 12(3):5-18.

35. **Giammanco M, Di Liegro CM, Schiera G and Di Liegro I (2020):** Genomic and Non-Genomic Mechanisms of Action of Thyroid Hormones and Their Catabolite 3,5-Diiodo-L-Thyronine in Mammals. International Journal of Molecular Sciences. 21(11):2-40.

36. **Kochman J, Jakubczyk, K, Bargiel, P and Janda-Milczarek K (2021):** The Influence of Oxidative Stress on Thyroid Diseases. Antioxidants. 10:2-11.

37. **Caporali S, De Stefano A, Calabrese C, Giovannelli A, Pieri M, Savini I (2022):** Anti-inflammatory and active biological properties of the plant-derived bioactive compounds luteolin and luteolin 7-glucoside. Nutrients. 14(6):1155.

38. Yahyazadeh A and Altunkaynak B (2019): Protective effects of luteolin on rat testis following exposure to 900 MHz electromagnetic field. Biotech Histochem 94: 298-307.

39. AL-Megrin WA, Alomar S, Alkhuriji AF, Metwally DM, Mohamed SK, Kassab RB, Abdel Moneim AE, El-Khadragy MF (2020): Luteolin protects against testicular injury induced by lead acetate by activating the Nrf2/HO-1 pathway. IUBMB Life 72: 1787-1798.

40. Akarsu S, Acısu T, Güngör İ, Cihangiroğlu C, Koca RH, Türk G, Sönmez M, Gür S, Fırat F and Durue HE (2023): The effect of luteolin on spermatological parameters, apoptosis, oxidative stress rate in freezing rabbit semen. Pol J Vet Sci:91-98-91-98.

41. Chen CY, Peng WH, Wu LC, Wu CC and Hsu SL (2010): Luteolin ameliorates experimental lung fibrosis both in vivo and in vitro: Implications for therapy of lung fibrosis. J. Agricultur. Food Chem. 58: 11653-11661.

42. Iman N, Mady B, and Solaiman A (2024): Evaluation of the probable alleviating effect of luteolin on acrylamide mediated toxicity of the caput epididymal lining epithelium in adult rats: Histological and biochemical study. Egyptian Journal of Histology 47.3 (2024): 991-1008.

فعالية اللوتولين في التخفيف من التغيرات الهيكلية فى البربخ الناتجة عن فرط نشاط الغدة الدرقية المستحث فى الجرذان البيضاء البالغة (دراسة نسيجية، مناعية نسيجية كميائية و قياسية)

إيناس أنور بخيت و هالة طه شعلان

قسم التشريح والأجنة، كلية الطب، جامعة عين شمس

الخلفية: يعتبر البربخ جزءًا من الجهاز التناسلي الذكري المسؤول عن تخزين وتطوير الحيوانات المنوية. و يُعرف فرط نشاط الغدة الدرقية بزيادة مستويات هرمونات الغدة الدرقية في الدم، و يمكن أن تؤثر التغيرات في مستوى هرمونات الغدة الدرقية سلبًا على مختلف الأعضاء وقد تؤدي إلى العقم.

الهدف: تهدف الدراسة الحالية إلى تقييم فعالية اللوتولين في التخفيف من التأثيرات الهيكلية فى البربخ الناتجة عن فرط نشاط الغدة الدرقية المستحث فى الجرذان البيضاء البالغة.

المواد والأساليب: تم تقسيم أربعين من ذكور الجرذان البيضاء البالغة إلى أربع مجموعات: المجموعة الأولى قسمت الى: المجموعة الفرعية الأولى : لم تتلق الجرذان أي علاج. المجموعة الفرعية الثانية: تم إعطاء كل جرذ ٠,٥ مل من زيت الزيتون عبر أنبوب معدي لمدة أربعة أسابيع. المجموعة الثانية: تم إعطاء كل جرذ ٥٠ ملغم/كجم من اللوتولين يوميًا عبر أنبوب معدي لمدة أربعة أسابيع. المجموعة الثالثة: تم إعطاء كل جرذ ١٠٠ ميكروجرام من ليفوثيروكسين لكل كجم من وزن الجسم يوميًا عبر أنبوب معدي لمدة أربعة أسابيع لتحفيز فرط النشاط الدرقي. المجموعة الرابعة: تم إعطاء كل جرذ ليفوثيروكسين كما في المجموعة الثالثة، بالإضافة إلى اللوتولين كما في المجموعة الثانية.

النتائج: أظهر البربخ في جرذان المجموعة الثالثة العديد من التغيرات التركيبية والدقيقة، مع زيادة ملحوظة في عدد الحيوانات المنوية المشوهة، وألياف الكولاجين، ومستويات هرمونات الغدة الدرقية (T٣ و T٤)، بالإضافة إلى زيادة في تعبير بروتينات PCNA وAR مقارنةً بالمجموعة الضابطة. بالمقابل، أظهر البربخ في جرذان المجموعة الرابعة خصائص قريبة من الطبيعية، مع زيادة في ألياف الكولاجين وهرمونات الغدة الدرقية. ومع ذلك، لم يكن هناك فرق كبير في عدد الحيوانات المنوية المشوهة أو تعبير بروتينات PCNA وAR مقارنةً بالمجموعة الضابطة.

الاستنتاج: قد يُعتبر اللوتولين مكملاً طبيعياً محتملاً لعلاج العقم عند الذكور، خاصة في الحالات المرتبطة بالإجهاد التأكسدي مثل فرط نشاط الغدة الدرقية.